

White matter microstructure throughout the brain correlates with visual imagery in grapheme–color synesthesia



Kirstie J. Whitaker^{a,*}, Xiaojian Kang^b, Timothy J. Herron^c, David L. Woods^{b,c,d,e},
Lynn C. Robertson^{c,f}, Bryan D. Alvarez^f

^a Department of Psychiatry, University of Cambridge, Cambridge CB2 0SZ, UK

^b Department of Neurology, University of California, Davis 4860 Y St., Suite 3700, Sacramento, CA 95817, USA

^c Medical Research Service, Veterans Administration, Martinez, CA 94553, USA

^d Center for Neurosciences, University of California, Davis, 1544 Newton Ct., Davis, CA 95616, USA

^e Center for Mind and Brain, University of California, Davis, 202 Cousteau Place, Suite 201, Davis, CA 95616, USA

^f Cognitive Neuropsychology Laboratory, University of California, Berkeley, CA 94720-5050, USA

ARTICLE INFO

Article history:

Accepted 23 December 2013

Available online 7 January 2014

ABSTRACT

In this study we show, for the first time, a correlation between the neuroanatomy of the synesthetic brain and a metric that measures behavior not exclusive to the synesthetic experience. Grapheme–color synesthetes ($n = 20$), who experience colors triggered by viewing or thinking of specific letters or numbers, showed altered white matter microstructure, as measured using diffusion tensor imaging, compared with carefully matched non-synesthetic controls. Synesthetes had lower fractional anisotropy and higher perpendicular diffusivity when compared to non-synesthetic controls. An analysis of the mode of anisotropy suggested that these differences were likely due to the presence of more crossing pathways in the brains of synesthetes. Additionally, these differences in white matter microstructure correlated negatively, and only for synesthetes, with a measure of the vividness of their visual imagery. Synesthetes who reported the most vivid visual imagery had the lowest fractional anisotropy and highest perpendicular diffusivity. We conclude that synesthetes as a population vary along a continuum while showing categorical differences in neuroanatomy and behavior compared to non-synesthetes.

© 2014 Elsevier Inc. All rights reserved.

Introduction

John Locke described the blending of senses that characterizes synesthesia in “An Essay Concerning Human Understanding” several centuries ago (Locke, 1689). Since that time, synesthesia has come to encompass a growing number of experientially-defined phenomena in which one cognitive domain (e.g., sounds, graphemes, language, emotions, etc.) triggers another domain automatically, consistently, and consciously. Grapheme–color synesthesia is one of the most closely studied and most common varieties, characterized by consistent and automatic experiences of color triggered when viewing or imagining graphemes (e.g., letters, numbers, etc.). Behavioral and brain-based research has led to a number of new understandings about synesthesia, although synesthesia is by definition a subjective experience and more work is needed to link the discoveries about brain mechanisms of synesthetes to their own elusive subjective experiences. In this study we examined how the white matter microstructure of grapheme–color synesthetes differs from that of non-synesthetes: both

categorically between the groups and in relation to a behavioral metric (visual imagery) not exclusive to synesthetic experience.

Brain-based models of grapheme–color synesthesia have commonly focused on the involvement of local cortical regions and networks such as visual area V4 in the origin of synesthetic color experience (Brang et al., 2010; Hubbard et al., 2005). While local regions of visual cortex likely do play a role in synesthetic neurophysiology some studies have failed to confirm the role of V4 in grapheme–color synesthesia (Hupé et al., 2012; Rich et al., 2006; Rouw and Scholte, 2007). Other neuroimaging studies (Esterman et al., 2006; Nunn et al., 2002; Rouw and Scholte, 2007; Sinke et al., 2012; Van Leeuwen et al., 2010; Weiss and Fink, 2009) have suggested a critical role of the parietal and frontal regions in the integration and binding of the components of synesthetic percepts, and recent studies suggest the involvement of highly distributed cortical areas in the synesthetic representation (Dovern et al., 2012; Hänggi et al., 2011; Hupé et al., 2012) particularly involving fronto-parietal networks. The prefrontal and parietal cortices have been linked with a multitude of behaviors, and are best described as *association cortex*, receiving inputs from all regions of the brain (Hagmann et al., 2008). Seen in this context, is not surprising that synesthetes would demonstrate differences in these networks, because

* Corresponding author.

E-mail address: kw401@cam.ac.uk (K.J. Whitaker).

synesthetic perception combines information from multiple cognitive and perceptual domains.

The white matter connections between different brain regions can be analyzed with diffusion tensor imaging (DTI). Water diffuses preferentially along axons rather than perpendicular to them, particularly for myelinated axons in a coherent fiber tract (Assaf and Pasternak, 2008; Beaulieu, 2002). Diffusion-weighted MRI is sensitive to the direction of water movement and, after fitting this movement to a tensor model, several measures are commonly extracted. Fractional anisotropy (FA), a scaled ratio of the propensity of water to diffuse along axon bundles (parallel diffusivity, λ_1) versus across them (perpendicular diffusivity, λ_{23}), is a proxy measure of white matter microstructure (Basser, 1995; Basser and Pierpaoli, 1996). Mean diffusivity (MD) is the average of diffusion in all three orthogonal directions. We hypothesized that synesthetes would demonstrate globally distributed differences in these measures of water diffusion due to differences in their underlying white matter microstructure.

If grapheme–color synesthesia reflects widespread differences in the distributed neural network architecture, it would be expected that synesthetes would show other differences in perceptual processing beyond their specific synesthetic experiences. Indeed, grapheme–color synesthetes show widely distributed increases in stimulus-evoked neural activity when tested via electroencephalography (EEG, Barnett et al., 2008; Jäncke & Langer, 2011; Volberg et al., 2013) and fMRI (Dovern et al., 2012; Hänggi et al., 2011; Hupé et al., 2012), along with increased cross-modal interactions (vision and audition) in response to stimuli that do not induce synesthetic color (Brang et al., 2012, but see Neufeld et al., 2012 for a contrary finding). Relative to matched controls, grapheme–color synesthetes also show increased excitability in the primary visual cortex (Terhune et al., 2011), more accurate color discrimination (Yaro and Ward, 2007), better memory (Smilek et al., 2002; Yaro and Ward, 2007), stronger visual imagery (Barnett and Newell, 2008) and heightened creativity (Mulvenna et al., 2003; Ward et al., 2008). With the possible exception of color discrimination, these factors do not rely specifically on color-selective area V4 or any other single neural locus implied specifically in a synesthetic experience.

If specific and unimodal forms of synesthesia such as grapheme–color reflect a broadly distributed pattern of neural activity and anatomy, one might expect to find a correlative behavioral metric that is equally broad, while also being unique in some way to synesthesia. Rouw and Scholte (2007) offer a piece of critical evidence, showing that grapheme–color synesthetic experience can be matched with differences in white matter microstructure. In this study we pursued this finding further, asking whether proxy measures of white matter microstructure obtained using diffusion tensor imaging would correlate with the vividness of visual imagery (VVI, Marks, 1973) which is typically enhanced in synesthetic subjects (Barnett and Newell, 2008).

Visual imagery is the ability to “see in the mind’s eye” when there are no external stimuli present. Connections between synesthesia and imagery were proposed early on (Ramachandran and Hubbard, 2001) and have been substantiated in synesthetes (Barnett and Newell, 2008; Price, 2009). Most synesthetes have vivid visual imagery. For example, grapheme–color synesthesia can be triggered simply by imagining a grapheme when a physical stimulus is not present (Elias et al., 2003; Jansari et al., 2006; Spiller and Jansari, 2008).

Here, we address the degree to which differences in white matter microstructure in grapheme–color synesthetes are categorically different to non-synesthete controls, and whether the differences correlate with a behavioral measure that is not unique to synesthesia *per se*. We first seek to replicate previous studies showing that synesthetes have more vivid visual imagery than closely-matched, non-synesthete controls. We then test whether synesthetes show differences in white matter microstructure compared with yoked controls as has been shown in the past (Rouw and Scholte, 2007).

Finally, we investigate the relationship between VVI and white matter microstructure in both the synesthetic and control populations to see how a cognitively distributed behavior such as mental imagery (Mechelli et al., 2004) correlates with global differences in neuroanatomy.

Methods

Participants

Twenty grapheme–color synesthetes and twenty non-synesthete controls participated in this study. All participants had normal or corrected to normal vision, no reported history of neurological or psychiatric disorder, and gave signed informed consent before entering the study as approved by the institutional review board of Veterans Affairs. Synesthesia was verified with the Online Synesthesia Battery (Eagleman et al., 2007) and an in-person interview with an expert in synesthesia (BA). Only those who showed consistent and conscious experience of grapheme–color synesthesia and scored less than 1 on the Synesthesia Battery ($M = 0.64$, $SD = 0.14$, range of scores = 0.58 to 0.9) were considered eligible as synesthetic subjects, although several grapheme–color synesthetes also reported other forms of synesthesia. Non-synesthete controls also participated in the interview to assure that they experienced none of the various forms of synesthesia. The participants were paid \$12 per hour for participation.

Synesthetes and controls were meticulously matched for sex, age, handedness, and years of education, all of which can influence neuroanatomy. All participants were between the ages of 19 and 35 ($M = 25.8$, $SD = 4.1$, 34 female) and between 14 and 24 years of education ($M = 18.1$, $SD = 2.3$). Each control was yoked to a synesthete of the same sex, handedness, age, and years of education.

Visual imagery assessment

All subjects completed the Vividness of Visual Imagery Questionnaire (Marks, 1973). This questionnaire consists of 4 sets of 4 questions (16 in total), asking the participant to imagine specific scenarios relating to a topic, first with their eyes open and then with their eyes closed. The subjective report of the vividness of visual imagery is rated by the participant on a 5 point Likert scale where a score of 1 indicates the imagined image is “perfectly clear and as vivid as normal vision” and a score of 5 indicates “no image at all, you only ‘know’ that you are thinking of an object”. These scores were scaled to range between 0 and 1, with 1 representing the “best” visual imagery and 0 representing very poor visual imagery to allow the correlation analyses presented in the results section to be more easily understood. The test is undertaken twice: once with eyes open and again when eyes are closed. Since there was no significant difference between the scores for eyes open or eyes closed, the rest of our analyses focused on the average of each participant’s scores.

Diffusion tensor imaging data acquisition and preprocessing

Brain imaging data was collected at the Veterans Affairs Clinic in Martinez, California on a 1.5 T Eclipse Phillips MR scanner using a 4-channel head coil with a maximum gradient strength of 40 mT/m. Each participant underwent four sets of cardiac-gated DTI scans using echo-planar imaging (EPI; TR depends on the participant’s heart rate; $TE = 115.6$ ms; 3 mm^3 isotropic voxels). Two non-diffusion-weighted image and 6 diffusion-weighted directions were acquired per set, with a b-value of 1000 s/mm^2 . A T1-weighted image was also acquired in each participant for image registration ($TR = 15$ ms; $TE = 4.47$ ms; voxel size $1.3 \times 0.94 \times 0.94 \text{ mm}^3$).

Analyses were performed using tools from FDT (for Functional MRI of the Brain (FMRIB) Diffusion Toolbox, part of FSL 4.1) (Smith et al., 2004; Woolrich et al., 2009). Brain volumes were skull stripped using

the Brain Extraction Tool (Smith, 2002) and a 12 parameter affine registration to the non-diffusion weighted volume was applied to correct for head motion and eddy current distortions introduced by the gradient coils. A diffusion tensor model was fitted to the data in a voxel-wise fashion to generate whole brain maps of the three orthogonal eigenvectors and eigenvalues, mean diffusivity (MD), and fractional anisotropy (FA). We refer to the largest eigenvalue (λ_1) as *parallel diffusivity* and the average of the two remaining eigenvalues as *perpendicular diffusivity* (λ_{23}).

A white matter mask was created from each participant's high resolution T1-weighted scan, after brain extraction, using FAST (FMRIB's Automated Segmentation Tool, Zhang et al., 2001) which segments the brain into gray matter, white matter, and cerebral spinal fluid. This mask was transformed into the participant's DTI space by applying the inverse of the affine registration of the non-diffusion weighted volume to the high resolution image. Both the registration and calculations of the inverse transform used FLIRT (FMRIB's Linear Image Registration Tool, Jenkinson et al., 2002). This mask is an independent definition of white matter voxels in the FA map created from the DTI acquisition.

Finally, each of the participants' FA maps was aligned into standard space using FNIRT (FMRIB's Nonlinear Image Registration Tool, Andersson et al., 2007a, 2007b). By applying the same transform, mean diffusivity, parallel and perpendicular diffusivity, and the white matter mask were also transformed into standard space.

DTI analyses: tract-based spatial statistics

We performed voxel-wise statistical analysis using TBSS (Tract-Based Spatial Statistics, Smith et al., 2006). After FA maps were aligned to standard space, the mean FA image was generated and thinned to produce a mean FA skeleton that represented the centers of all tracts common to the group. Each subject's aligned FA, λ_1 , λ_{23} , and MD data were then projected onto this skeleton by finding the nearest maximum FA value for the individual. This projection step aims to remove the effect of cross-subject spatial variability that remains after the non-linear registration. Voxel-wise cross-subject permutation-based non-parametric statistics were performed using randomization (Nichols and Holmes, 2002) with 5000 permutations and threshold-free cluster enhancement to correct for multiple comparisons at $P < .05$ (Smith and Nichols, 2009).

We conducted three specific statistical tests on each of the measures of white matter microstructure (FA, λ_1 , λ_{23} and MD) in turn. The first, a student's *T*-test on the difference of means between synesthetes and controls. Secondly, a Pearson's correlation between white matter microstructure and average VVI for the whole group, and for each group separately. Finally, we looked for regions in which the correlation between VVI and white matter microstructure was significantly different for synesthetes and controls, controlling for differences in mean white matter measures.

We also used a recently developed tensor metric to identify regions of crossing fibers (Douaud et al., 2011): the mode of anisotropy (Ennis and Kindlmann, 2006). Regions with a positive mode have linear anisotropy, and are likely to be part of a highly directional tract. In contrast, regions with a low or negative mode can be described as having planar anisotropy, and are more likely to contain crossing fibers. We extracted mode values from voxels that were significantly different between synesthetes and non-synesthete controls. Specifically, we extracted mode values from the voxel whose value was projected onto the TBSS skeleton using the non-linear warping described above. Histograms with a bin width of 0.02 were created using fsIstats, an FSL tool (Smith, 2002). We used a Mann–Whitney *U*-test to compare the distributions of mode values within these results for synesthetes and non-synesthete controls.

Results

Behavioral differences in visual imagery

All participants completed the Vividness of Visual Imagery Questionnaire (Marks, 1973) by rating a series of questions about their own imagery. All scores were scaled between 0 and 1, where a score of 1 represents imagery as vivid as perception, and a score of 0 represents little to no mental imagery. As shown in Fig. 1, we replicated previous findings that grapheme–color synesthetes have more vivid visual imagery than non-synesthetes (*Student's T*(38) = 2.53, $P < 0.05$, two-tailed).

Group differences in white matter microstructure

We investigated voxel-based measures of white matter microstructure throughout the brain for all participants using diffusion tensor imaging. We conducted student's *t* tests to look for differences in mean value for four measures of white matter microstructure (FA, λ_1 , λ_{23} and MD). We found significant differences in FA and λ_{23} throughout the brain (Fig. 2), with synesthetes having lower FA and higher λ_{23} than non-synesthete controls. No group differences were found in λ_1 or MD, and no regions showed higher FA or lower λ_{23} for synesthetes when compared to non-synesthete controls. Table 1 lists the percentage of each white matter region of interest within the Johns Hopkins University (JHU) White Matter Label Atlas (Mori et al., 2005) that showed significant differences between synesthetes and controls.

To better characterize the anatomy of the white matter regions that were different between synesthetes and controls we investigated the mode of anisotropy, a recently developed tensor index (Ennis and Kindlmann, 2006) that can be used to identify regions of crossing fibers. We extracted the mode from every voxel on the white matter skeleton that showed significant differences between synesthetes and controls for every subject and plotted their distributions (Fig. 3). This method of investigating mode anisotropy has been successfully implemented in non-synesthetic human participants (Mackey et al., 2012), and we apply it here for the first time to a synesthetic population. Synesthetes had a significantly lower median mode (Mann–Whitney $U = 2.01 \times 10^{11}$, $df = 129816$, $P < .001$, two-tailed) when compared to non-synesthete controls.

Correlations between visual imagery and white matter

We next conducted a Pearson's correlation between VVI scores and DTI measures of white matter microstructure in order to investigate

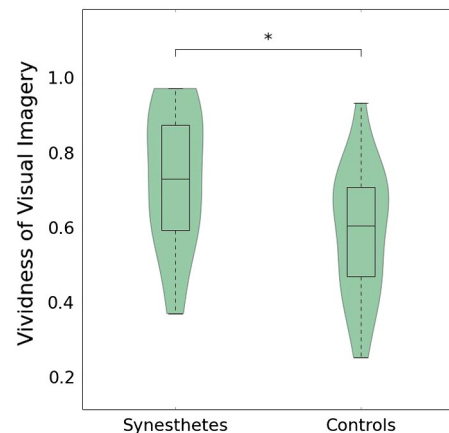


Fig. 1. Differences in vividness of visual imagery score between synesthetes and non-synesthetic matched controls. Synesthetes had significantly higher VVI scores than controls. The box is delimited by the 1st and 3rd quartiles of the data and split horizontally at the median point. Whiskers illustrate the highest and lowest data points that are within 1.5 times the interquartile range. The distribution of the data is shown in green via a kernel density estimate of the probability density function per data point.

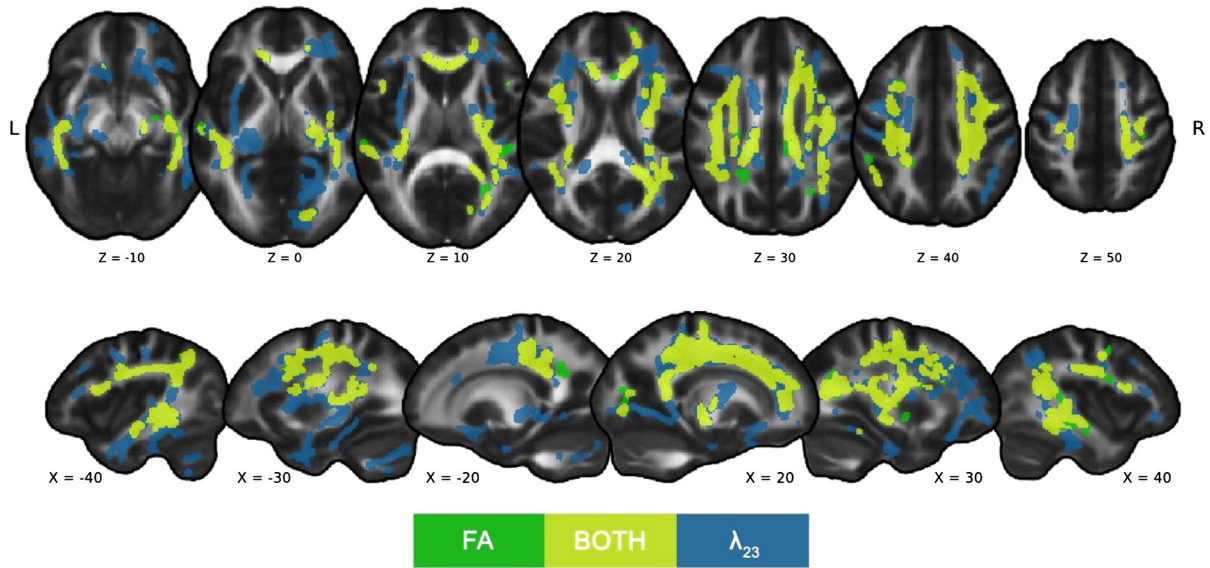


Fig. 2. Whole brain results of TBSS analysis showing significant differences between synesthetes and non-synesthete controls. Synesthetes had significantly lower fractional anisotropy (FA, green) and higher perpendicular diffusivity (λ_{23} , blue) in many regions through the brain. Regions in which both results were significant are shown in yellow. All analyses were performed on the white matter skeleton; results were filled for easier visualization.

the individual differences in brain and behavior. As shown in Fig. 4, we found a strong negative correlation between VVI and FA throughout the brain for all participants. This was accompanied by a strong positive correlation with λ_{23} . The percentage of each white matter region of interest from the JHU atlas (Mori et al., 2005) that showed significant correlations between FA, λ_{23} , or both, and VVI is tabulated in Table 2.

Given the group differences in both brain (Fig. 2) and behavior (Fig. 1), we chose to investigate correlations in the two groups separately. We saw strong correlations between VVI and white matter structure

in synesthetes (negative correlation with FA, positive correlation with λ_{23} , Fig. 5 and Table 2), concentrated in the white matter projecting to the association cortex. In contrast, we found no significant results in non-synesthete controls. In order to visualize the correlation, we extracted average FA from every voxel which showed a significant correlation with either FA or λ_{23} when synesthetes were examined alone (Fig. 5), and for both synesthetes and controls. Fig. 5B illustrates the negative correlation between FA and VVI for synesthetes used to define the ROI. Average FA from the same voxels in the control participants

Table 1

Regions of the JHU White Matter Label Atlas that show significant differences between synesthetes and non-synesthete control participants. The number of voxels in the white matter skeleton that fall in each label is listed along with the percentage of these voxels that show significant differences in FA, λ_{23} , and both measures.

White Matter Labels	Voxels in white matter skeleton	Group differences (% of skeleton)		
		FA	L23	Both
Body of corpus callosum	3217	192	31.5	176
Splenium of corpus callosum	2648	103	25.1	81
Genu of corpus callosum	1789	11.6	43.1	65
Fornix	786	31.6	38.2	299
L anterior corona radiata	1800	7.2	8.3	7.2
R anterior corona radiata	1721	25.6	40.7	24.5
L superior corona radiata	1354	31.9	56.9	287
R superior corona radiata	1362	24.6	67.8	21.1
L posterior corona radiata	748	23.0	49.2	166
R posterior corona radiata	846	20.2	51.9	171
L superior longitudinal fasciculus	1450	166	54.4	126
R superior longitudinal fasciculus	1514	20.4	63.5	15.2
L superior fronto-occipital fasciculus	100	28.0	28.0	28.0
R superior fronto-occipital fasciculus	113	0.0	0.0	0.0
L uncinata fasciculus	65	0.0	0.0	0.0
R uncinata fasciculus	69	39.1	39.1	39.1
L posterior thalamic radiation	1103	9.3	16.4	8.9
R posterior thalamic radiation	1141	15.2	35.4	11.7
L cingulum	661	1.47	21.9	13.3
R cingulum	716	1.35	23.6	11.5
L sagittal stratum	489	33.5	66.7	32.5
R sagittal stratum	576	2.03	42.2	10.9
L internal capsule	2367	7.5	1.42	5.9
R internal capsule	2484	1.47	36.3	12.0
L external capsule	1443	31.3	31.8	30.8
R external capsule	1302	1.83	27.7	12.7
Cerebellum	4273	5.7	5.7	5.7
Brainstem	2490	1.81	1.92	1.80
Not classified	157,763	11.5	21.6	20.9

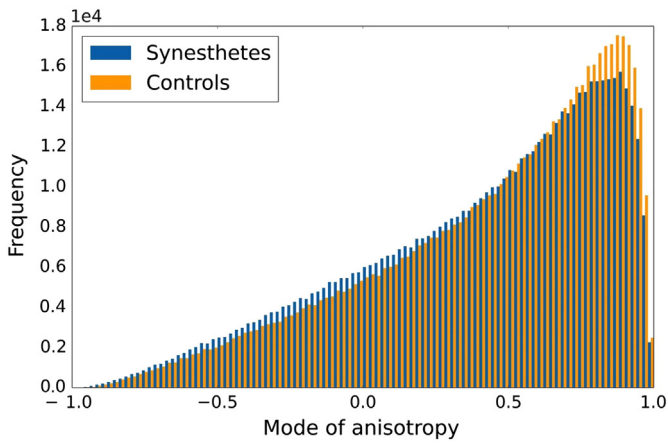


Fig. 3. Distributions of mode values within voxels showing differences in white matter microstructure between controls and synesthetes. Synesthetes have a significantly lower median mode which is indicative of less coherent white matter tracts in these regions.

showed no correlation ($r^2 = 0.004$, $P = 0.79$, Fig. 5B). Since it is difficult to interpret the lack of significant results in the control group, we tested the difference in correlations for synesthetes and non-synesthete controls. We found several regions for which the positive correlation between VVI and λ_{23} was stronger in synesthetes than controls: bilateral posterior corona radiata, left superior corona radiata, and the body of the corpus callosum (Fig. 5). There were no regions that showed a significantly larger correlation in synesthetes than controls for FA.

Discussion

This study is the first to provide evidence that grapheme–color synesthetes show a correlation between globally distributed differences in white matter microstructure and the vividness of visual imagery. Synesthetes show significantly lower FA throughout the white matter and statistically higher scores on the test of the vividness of visual imagery. These lower global FA and higher average VVI scores are corroborated by a significant negative correlation unique to synesthetes between FA and VVI: synesthetes with the lowest FA have the most vivid visual imagery.

Reports of neuroanatomical differences in grapheme–color synesthetes are increasingly common (Dover et al., 2012; Hänggi et al.,

2011; Hupé et al., 2012; Jäncke et al., 2009; Rouw and Scholte, 2007). Moreover, new studies of the brains of grapheme–color synesthetes report widely distributed differences in anatomical structure (Hupé et al., 2012), in hyperconnectivity (Hänggi et al., 2011) and in functional resting-state connectivity (Dover et al., 2012), regardless of the unresolved inconsistencies in the direction of difference.

Our study is the first to investigate the mode of anisotropy in synesthetes which describes the type of anisotropy: linear or planar. Water diffusion through crossing fibers will typically result in planar anisotropy, which is represented by more negative mode values. In contrast, diffusion in a single direction (e.g., along a non-decussated fiber bundle) will result in linear anisotropy, represented by more positive mode values. We show that the regions with lower FA and higher λ_{23} also have lower mode values in synesthetes compared to controls. Douaud et al. (2011) have shown higher FA and mode values in older adults with mild cognitive impairment (MCI) compared to age-matched controls in the centrum semiovale which contains crossing fiber tracts. They suggest that as one tract deteriorates, the mode and FA increase because white matter coherence in the remaining tract is more clearly revealed. This leads us to interpret the differences between synesthetes and non-synesthete controls as due to less coherent white matter structure throughout the brain rather than reduced myelination. The axons in the synesthetes' brains are going in different directions, and connecting more disparate regions of cortex.

The results presented in the current study further validate findings showing widely distributed differences in white matter microstructure throughout the brain. It is of particular note that the regions in which we see the strongest correlation between white matter microstructure and VVI (Fig. 5) are tracts near the association cortex, the axons from which, by definition, project to and from many different cortical targets. The parietal cortex in particular is ubiquitous to both synesthetic neuro-anatomical findings and associative processing in general due to its role as a hub of cortical and subcortical interconnectivity in the human brain (Hagmann et al., 2008). It is possible that grapheme–color synesthesia represents differences in parietal function (Specht and Laeng, 2011). Given the widespread connectivity of the parietal lobe, which is thought to play a role in binding synesthetic color in synesthetes (Esterman et al., 2006; Robertson, 2003), and the fact that grapheme–color synesthetes show some advantage beyond their synesthetic modalities alone, we looked beyond synesthetic experience to examine relationships between behavioral and neuroanatomical differences in this population. Grapheme–color synesthetes in the present study have

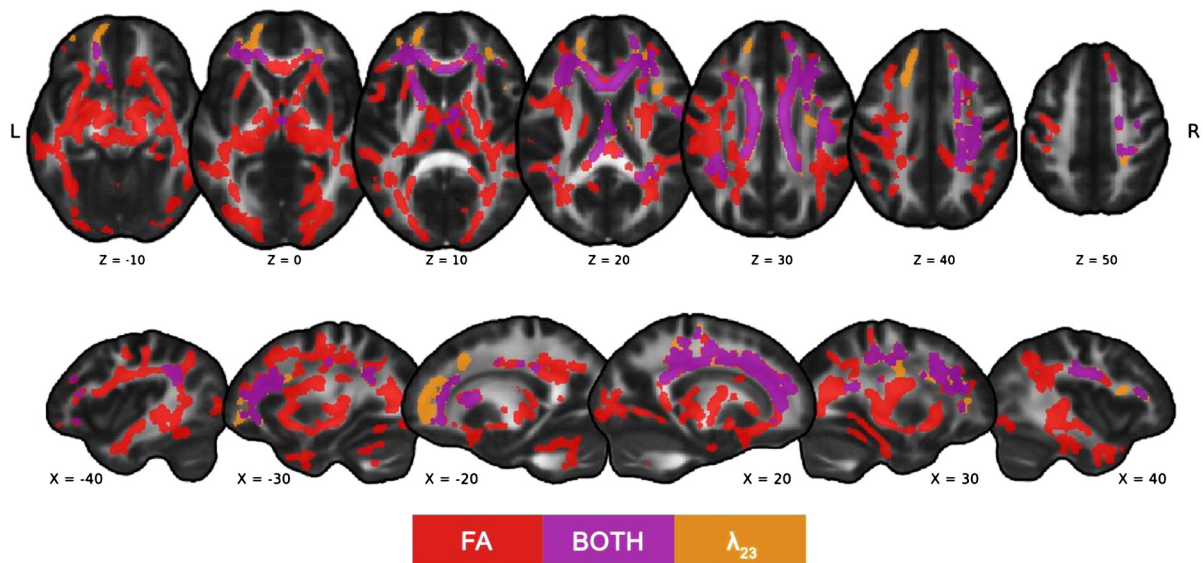


Fig. 4. Whole brain results of TBSS analysis showing significant correlations between VVI and FA (negative, red) or λ_{23} (positive, orange) in all participants. Regions in which both results were significant are shown in purple. All analyses were performed on the white matter skeleton; results were filled for easier visualization.

Table 2

Regions of the JHU White Matter Label Atlas that show significant correlations between VVI and FA, λ_{23} or both measures of white matter microstructure. The number of voxels in the white matter skeleton in each label is listed in Table 1 and the percentage of these voxels that show significant correlations with FA, λ_{23} and both measures are shown for the analysis of all participants (Fig. 4) and synesthetes alone (Fig. 5).

White matter labels	Correlation with WI					
	All participants (% of skeleton)			Synesthetes only (% of skeleton)		
	FA	L23	Both	FA	L23	Both
Body of corpus callosum	22.8	57.6	1.5	15.5	46.3	8.6
Splenium of corpus callosum	20.3	10.3	0.2	3.0	2.3	1.4
Genu of corpus callosum	29.5	30.6	0.7	9.7	20.0	0.8
Fornix	56.2	9.3	0.9	19.7	0.0	0.0
L anterior corona radiata	22.6	33.7	7.1	22.2	41.9	9.9
R anterior corona radiata	27.7	37.9	1.9	15.8	52.5	4.3
L superior corona radiata	30.5	2.9	0.4	24.8	26.1	8.6
R superior corona radiata	30.0	28.0	8.6	24.1	38.0	21.9
L posterior corona radiata	34.5	0.4	0.0	27.8	27.8	27.8
R posterior corona radiata	14.2	14.5	0.6	8.5	26.8	4.3
L superior longitudinal fasciculus	47.1	6.8	0.2	14.3	26.3	6.1
R superior longitudinal fasciculus	24.4	26.0	4.3	11.5	19.4	3.3
L superior fronto-occipital fasciculus	12.0	0.0	0.0	0.0	0.0	0.0
R superior fronto-occipital fasciculus	0.0	0.0	0.0	70.8	0.9	0.0
L uncinate fasciculus	87.7	0.0	0.0	26.2	52.3	0.0
R uncinate fasciculus	55.1	0.0	0.0	0.0	0.0	0.0
L posterior thalamic radiation	33.3	0.0	0.0	0.3	0.3	0.3
R posterior thalamic radiation	28.1	4.8	0.3	0.0	0.0	0.0
L cingulum	6.2	7.9	1.2	1.5	2.9	1.5
R cingulum	24.7	5.0	0.3	0.4	4.5	0.3
L sagittal stratum	44.2	0.0	0.0	0.0	0.0	0.0
R sagittal stratum	43.2	0.0	0.0	2.3	0.0	0.0
L internal capsule	19.3	6.6	0.2	3.6	0.3	0.0
R internal capsule	45.0	0.0	0.0	5.6	5.0	5.0
L external capsule	42.3	0.0	0.0	1.6	0.1	0.1
R external capsule	47.1	0.0	0.0	15.1	18.0	2.2
Cerebellum	20.4	0.0	0.0	0.0	0.0	0.0
Brainstem	39.9	0.0	0.0	0.0	0.0	0.0
Not classified	27.8	34.6	8.8	8.5	11.0	10.0

more vivid visual imagery than the matched controls, replicating a similar result reported by [Barnett and Newell \(2008\)](#). As seen in [Fig. 5](#), synesthetes show significant correlations with FA and λ_{23} and visual imagery through the fronto-parietal networks, but not within the early visual regions. As visual imagery becomes more vivid for synesthetes, white matter microstructure in the fronto-parietal networks decreases, becoming less like the non-synesthete control group. Individual differences that are not present in the white matter near the early visual cortex become apparent in tracts connecting the association cortices.

It is important to note that our interpretations of the relationships between our participants' neuroanatomy and their vividness of visual imagery or synesthetic experience are based on estimates from the diffusion tensor imaging; an inexact, proxy measure of the brain structure. We have interpreted differences in FA, λ_{23} and mode of anisotropy as differences in the connections between regions but this cannot be proven using diffusion weighted MRI of living humans. There are multiple biological factors that affect water diffusion, including but not limited to: fiber diameter, fiber density, membrane permeability, and myelination ([Beaulieu, 2002](#)). At this level of resolution it is not possible to differentiate between these possibilities, although alternative imaging techniques such as magnetization transfer contrast ([Wolff and Balaban, 1989](#)), and myelin water quantification ([MacKay et al., 1994](#)), have been proposed to further elucidate white matter structure. We hope that future studies of synesthesia, a perceptual phenomenon that cannot be investigated in animal models, build on the work presented here in order to clarify our inferences of the relationships between diffusion tensor measures, synesthetic experience and VVI.

Further studies are also needed to investigate the role of strategy differences for grapheme-color synesthetes on the relationship between white matter microstructure and VVI. It is possible that the negative correlation between FA and VVI observed here may be generated by the utilization of a different strategy for grapheme-color synesthetes. Synesthetes with vivid imagery/lower FA may rely on increasingly

visual-based imagery, whereas synesthetes that follow a pattern more similar to controls may show a more typical memory-based imagery. Additionally, synesthetes in this study have more vivid imagery and it is possible that this group difference in imagery accounts for the differences in white matter microstructure. Another study, which recruited and compared a control group who matched the synesthetes in their vividness of visual imagery, would elucidate the unique contribution of high VVI on the correlation we have observed only in the synesthetes in this study.

Conclusion

Grapheme-color synesthetes in this study show significantly lower fractional anisotropy and higher perpendicular diffusivity throughout much of the brain, and more vivid self-reported visual imagery when compared to a control group of non-synesthetes. Our investigation of the distribution of mode of anisotropy values within regions showing differences between the groups suggests that these are likely due to a higher degree of crossing fibers in synesthetes. A significant negative correlation between FA and visual imagery, specific to the synesthete population, was found: synesthetes with the lowest FA had the most vivid visual imagery. We have demonstrated a categorical difference between synesthetes and non-synesthete controls in both brain and behavior, and a continuum within the synesthetic population between neuroanatomical differences and their vividness of visual imagery.

Acknowledgments

We would like to thank Silvia Bunge, Anthony Cate, Francesca Fortenbaugh, Allison Leib, and Allison Connell for their support and helpful discussions. This research was supported by National Eye Institute Grant F31EY021446 (to B.D.A.) and a Veterans Administration and National Institutes of Health Grant MH-0164458 (to L.C.R.). Lynn

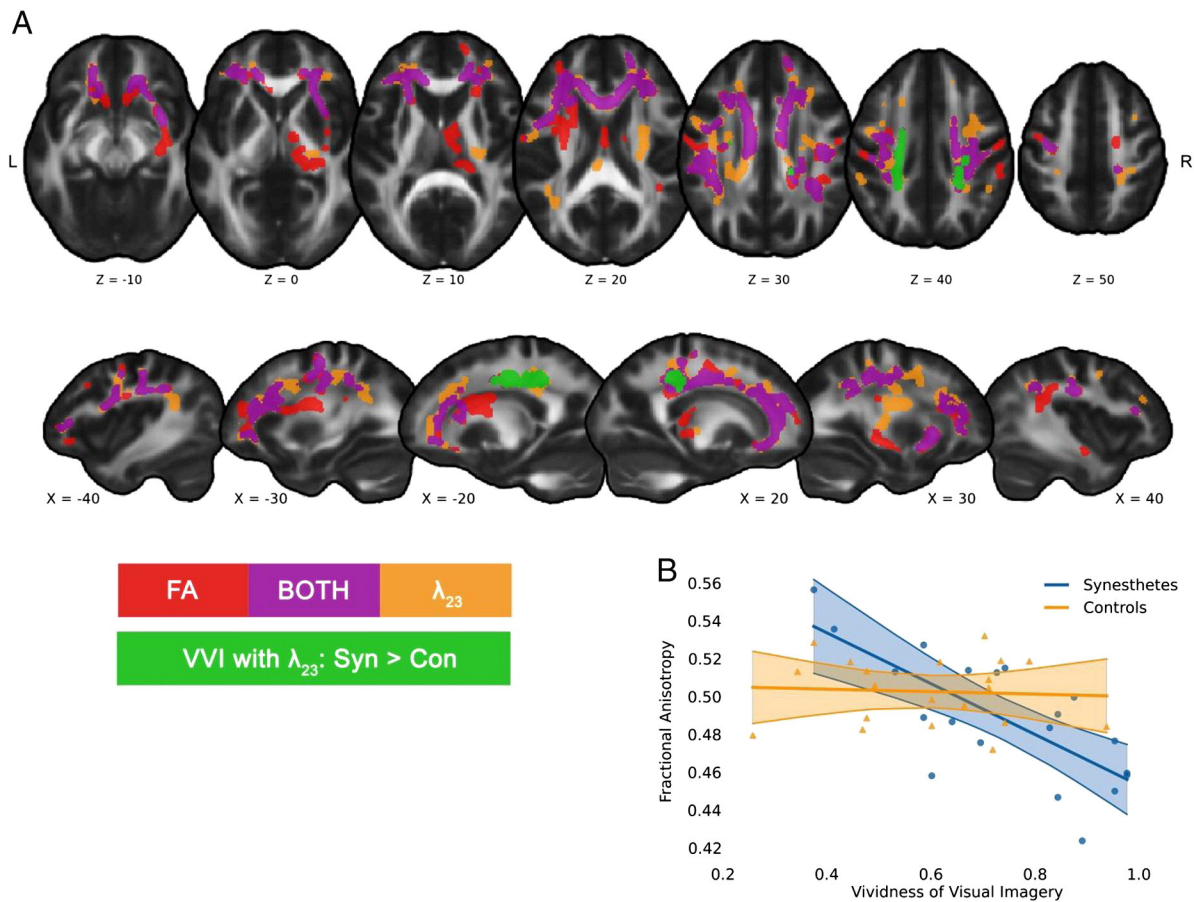


Fig. 5. A) Whole brain results of TBSS analysis showing significant correlations between VVI and FA (negative, red) or λ_{23} (positive, orange) in synesthetes alone. Regions in which both results were significant are shown in purple. Bright green tracts in the left and right corona radiata are those voxels for which the correlation in synesthetes is significantly larger than the correlation in non-synesthete controls. All analyses were performed on the white matter skeleton; results were filled for easier visualization. B) The correlation of average FA in all voxels of the white matter skeleton that show a significant relationship between FA and/or λ_{23} for synesthetes is plotted for visualization purposes only. Shaded regions represent the upper and lower 95% confidence intervals of the regression line. Synesthetes (blue) and non-synesthete controls (yellow) are plotted separately.

C. Robertson has a Senior Research Career Scientist award from the Veterans Administration and is affiliated with the VA Clinical Sciences Research Service, VA, Northern California Health Care System, Martinez, CA.

References

- Andersson, J.L.R., Jenkinson, M., Smith, S., 2007a. Non-linear registration, aka Spatial normalisation FMRIB technical report TR07JA2. FMRIB Analysis Group of the University of Oxford (at <http://www.fmrib.ox.ac.uk/analysis/techrep/tr07ja2/tr07ja2.pdf>).
- Andersson, J.L.R., Jenkinson, M., Smith, S., 2007b. Non-linear optimisation. In: FMRIB Technical Report TR07JA1. FMRIB Centre, Oxford (UK) (at <http://fsl.fmrib.ox.ac.uk/analysis/techrep/tr07ja1/tr07ja1.pdf>).
- Assaf, Y., Pasternak, O., 2008. Diffusion tensor imaging (DTI)-based white matter mapping in brain research: a review. *J. Mol. Neurosci.* 34, 51–61.
- Barnett, K.J., Newell, F.N., 2008. Synaesthesia is associated with enhanced, self-rated visual imagery. *Conscious. Cogn.* 17, 1032–1039.
- Barnett, K.J., et al., 2008. Differences in early sensory-perceptual processing in synesthesia: a visual evoked potential study. *Neuroimage* 43, 605–613.
- Basser, P.J., 1995. Inferring microstructural features and the physiological state of tissues from diffusion-weighted images. *NMR Biomed.* 8, 333–344.
- Basser, P.J., Pierpaoli, C., 1996. Microstructural and physiological features of tissues elucidated by quantitative-diffusion-tensor MRI. *J. Magn. Reson. B* 111, 209–219.
- Beaulieu, C., 2002. The basis of anisotropic water diffusion in the nervous system—a technical review. *NMR Biomed.* 15, 435–455.
- Brang, D., Hubbard, E.M., Coulson, S., Huang, M., Ramachandran, V.S., 2010. Magnetoencephalography reveals early activation of V4 in grapheme-color synesthesia. *Neuroimage* 53, 268–274.
- Brang, D., Williams, L.E., Ramachandran, V.S., 2012. Grapheme-color synesthetes show enhanced crossmodal processing between auditory and visual modalities. *Cortex* 48, 630.
- Douaud, G., et al., 2011. DTI measures in crossing-fibre areas: increased diffusion anisotropy reveals early white matter alteration in MCI and mild Alzheimer's disease. *Neuroimage* 55, 880–890.
- Dovern, A., et al., 2012. Intrinsic network connectivity reflects consistency of synesthetic experiences. *J. Neurosci.* 32, 7614–7621.
- Eagleman, D.M., Kagan, A.D., Nelson, S.S., Sagaram, D., Sarma, A.K., 2007. A standardized test battery for the study of synesthesia. *J. Neurosci. Methods* 159, 139–145.
- Elias, L.J., Saucier, D.M., Hardie, C., Sarty, G.E., 2003. Dissociating semantic and perceptual components of synaesthesia: behavioural and functional neuroanatomical investigations. *Cogn. Brain Res.* 16, 232–237.
- Ennis, D.B., Kindlmann, G., 2006. Orthogonal tensor invariants and the analysis of diffusion tensor magnetic resonance images. *Magn. Reson. Med.* 55, 136–146.
- Esterman, M., Verstynen, T., Ivry, R.B., Robertson, L.C., 2006. Coming unbound: disrupting automatic integration of synesthetic color and graphemes by transcranial magnetic stimulation of the right parietal lobe. *J. Cogn. Neurosci.* 18, 1570–1576.
- Hagmann, P., et al., 2008. Mapping the structural core of human cerebral cortex. *PLoS Biol.* 6, e159.
- Hänggi, J., Wotruba, D., Jäncke, L., 2011. Globally altered structural brain network topology in grapheme-color synesthesia. *J. Neurosci.* 31, 5816–5828.
- Hubbard, E., Arman, C., Boynton, G.M., Rama, V.S., 2005. Individual differences among grapheme-color synesthetes: brain-behavior correlations. *Neuron* 45, 975–985.
- Hupé, J.-M., Bordier, C., Dojat, M., 2012. The neural bases of grapheme-color synesthesia are not localized in real color-sensitive areas. *Cereb. Cortex* 22, 1622–1633.
- Jäncke, L., Langer, N., 2011. A strong parietal hub in the small-world network of coloured-hearing synesthetes during resting state EEG. *J. Neuropsychol.* 5 (2), 178–202.
- Jäncke, L., Beeli, G., Eulig, C., Hänggi, J., 2009. The neuroanatomy of grapheme-color synesthesia. *Eur. J. Neurosci.* 29, 1287–1293.
- Jansari, A.S., Spiller, M.J., Redfern, S., 2006. Number synaesthesia: when hearing 'four plus five' looks like gold. *Cortex* 42, 253–258.
- Jenkinson, M., Bannister, P., Brady, M., Smith, S., 2002. Improved optimization for the robust and accurate linear registration and motion correction of brain images. *Neuroimage* 17, 825–841.
- Locke, J., 1689. *An Essay Concerning Human Understanding* (Book III, Chapter IV, Section 11).
- MacKay, A., Whittall, K., Adler, J., Li, D., Paty, D., Graeb, D., 1994. In vivo visualization of myelin water in brain by magnetic resonance. *Magn. Reson. Med.* 31 (6), 673–677.
- Mackey, A.P., Whitaker, K.J., Bunge, S.A., 2012. Experience-dependent plasticity in white matter microstructure: reasoning training alters structural connectivity. *Front. Neuroanat.* 6.

- Marks, D.F., 1973. Visual imagery differences in the recall of pictures. *Br. J. Psychol.* 64, 17–24.
- Mechelli, A., Price, C.J., Friston, K.J., Ishai, A., 2004. Where bottom-up meets top-down: neuronal interactions during perception and imagery. *Cereb. Cortex* 14, 1256–1265.
- Mori, S., Wakana, S., Van Zijl, P.C.M., Nagae-Poetscher, L.M., 2005. *MRI Atlas of Human White Matter*. 1st ed. Elsevier.
- Mulvenna, C.M., Hubbard, E.M., Ramachandran, V.S., Pollick, F., 2003. The relationship between synaesthesia and creativity. http://sites.google.com/site/edhubbard/Mulvenna_CNS04.pdf.
- Neufeld, J., Sinke, C., Zedler, M., Emrich, H.M., Szycik, G.R., 2012. Reduced audio-visual integration in synaesthetes indicated by the double-flash illusion. *Brain Res.* 1473, 78–86. <http://dx.doi.org/10.1016/j.brainres.2012.07.011>.
- Nichols, T.E., Holmes, A.P., 2002. Nonparametric permutation tests for functional neuroimaging: a primer with examples. *Hum. Brain Mapp.* 15, 1–25.
- Nunn, J.A., et al., 2002. Functional magnetic resonance imaging of synesthesia: activation of V 4/V 8 by spoken words. *Nat. Neurosci.* 5, 371–375.
- Price, M.C., 2009. Spatial forms and mental imagery. *Cortex* 45, 1229–1245.
- Ramachandran, V.S., Hubbard, E.M., 2001. Psychophysical investigations into the neural basis of synaesthesia. *Proc. R. Soc. London, Ser. B* 268, 979–983.
- Rich, A.N., Williams, M.A., Puce, A., Syngeniotis, A., Howard, M.A., McGlone, F., Mattingley, J.B., 2006. Neural correlates of imagined and synaesthetic colours. *Neuropsychologia* 44, 2918–2925.
- Robertson, L.C., 2003. Binding, spatial attention and perceptual awareness. *Nat. Rev. Neurosci.* 4, 93.
- Rouw, R., Scholte, H.S., 2007. Increased structural connectivity in grapheme-color synesthesia. *Nat. Neurosci.* 10, 792–797.
- Sinke, C., Neufeld, J., Emrich, H.M., Dillo, W., Bleich, S., Zedler, M., Szycik, G.R., 2012. Inside a synesthete's head: a functional connectivity analysis with grapheme-color synesthetes. *Neuropsychologia* 50 (14), 3363–3369. <http://dx.doi.org/10.1016/j.neuropsychologia.2012.09.015>.
- Smilek, D., Dixon, M.J., Cudahy, C., Merikle, P.M., 2002. Synesthetic color experiences influence memory. *Psychol. Sci.* 13, 548–552.
- Smith, S.M., 2002. Fast robust automated brain extraction. *Hum. Brain Mapp.* 17, 143–155.
- Smith, S.M., Nichols, T.E., 2009. Threshold-free cluster enhancement: addressing problems of smoothing, threshold dependence and localisation in cluster inference. *Neuroimage* 44, 83–98.
- Smith, S.M., et al., 2004. Advances in functional and structural MR image analysis and implementation as FSL. *Neuroimage* 23, S208.
- Smith, S.M., et al., 2006. Tract-based spatial statistics: voxelwise analysis of multi-subject diffusion data. *Neuroimage* 31, 1487–1505.
- Specht, K., Laeng, B., 2011. An independent component analysis of fMRI data of grapheme-color synaesthesia. *J. Neuropsychol.* 5, 203–213.
- Spiller, M.J., Jansari, A.S., 2008. Mental imagery and synaesthesia: is synaesthesia from internally-generated stimuli possible? *Cognition* 109, 143–151.
- Terhune, D.B., Tai, S., Cowey, A., Popescu, T., Cohen Kadosh, R., 2011. Enhanced cortical excitability in grapheme-color synesthesia and its modulation. *Curr. Biol.* 21, 2006–2009.
- Van Leeuwen, T.M., Petersson, K.M., Hagoort, P., 2010. Synaesthetic colour in the brain: beyond colour areas. A functional magnetic resonance imaging study of synaesthetes and matched controls. *PLoS ONE* 5 (8), e12074.
- Volberg, G., Karmann, A., Birkner, S., Greenlee, M.W., 2013. Short- and long-range neural synchrony in grapheme-color synesthesia. *J. Cogn. Neurosci.* 25 (7), 1148–1162. http://dx.doi.org/10.1162/jocn_a_00374.
- Ward, J., Thompson-Lake, D., Ely, R., Kaminski, F., 2008. Synaesthesia, creativity and art: what is the link? *Br. J. Psychol.* 99, 127–141.
- Weiss, P.H., Fink, G.R., 2009. Grapheme-color synaesthetes show increased grey matter volumes of parietal and fusiform cortex. *Brain* 132, 65–70.
- Wolff, S.D., Balaban, R.S., 1989. Magnetization transfer contrast (MTC) and tissue water proton relaxation in vivo. *Magn. Reson. Med.* 10 (1), 135–144.
- Woolrich, M.W., et al., 2009. Bayesian analysis of neuroimaging data in FSL. *Neuroimage* 45, S173–S186.
- Yaro, C., Ward, J., 2007. Searching for Shereshevskii: what is superior about the memory of synaesthetes? *Q. J. Exp. Psychol.* 60, 681–695.
- Zhang, Y., Brady, M., Smith, S., 2001. Segmentation of brain MR images through a hidden Markov random field model and the expectation-maximization algorithm. *IEEE Trans. Med. Imaging* 20, 45–57.